

A hybrid method of solving near-zone composite electromagnetic scattering from targets and underlying rough surface*

Xi-Min Li(李西敏)^{1,†}, Jing-Jing Li(李晶晶)¹, Qian Gao(高乾)², and Peng-Cheng Gao(高鹏程)³

¹Air Force Engineering University, Xi'an 710051, China

²Air Force Communication NCO Academy, Dalian 116199, China

³Science and Technology on Electromagnetic Scattering Laboratory, Shanghai 200438, China

(Received 25 July 2019; revised manuscript received 27 October 2019; accepted manuscript online 5 December 2019)

For composite electromagnetic (EM) scattering from rough surface and target above it in near-field condition, modified shooting and bouncing ray (SBR) method and integral equation method (IEM), which are analytic methods combined with two-scale model for rough surface, are proposed to solve the composite near-field scattering problems. And the modified method is verified in effectiveness and accuracy by comparing the simulation results with measured results. Finally, the composite near-field scattering characteristics of a slanted plane and rough water surface below are obtained by using the proposed methods, and the dynamic tendency of composite scattering characteristics *versus* near-fielding distance is analyzed, which may have practical contribution to engineering programs in need of radar targets near-field characteristics under extra-low-altitude conditions.

Keywords: near-field scattering, rough surface, target in extra-low-altitude, shooting and bouncing ray (SBR)

PACS: 42.68.Mj, 42.68.Ay, 42.25.Bs, 42.15.Dp

DOI: 10.1088/1674-1056/ab5ef9

1. Introduction

The characteristics of extra-low-altitude targets and the environment around targets have great value in areas of missile-borne radar detecting in extra-low-altitude, air-borne radar detecting, and identification towards earth ground. Electromagnetic (EM) scattering from targets in extra-low-altitude and environments could be abstracted into scattering problems of radar targets above rough surface. The conventional far-field scattering from rough surface and targets has been widely investigated in the past decades,^[1-4] but research on near-field scattering from targets and surface has rarely been reported yet, which is really a hot topic and challenging issue. The near-field scattering from targets in free space is computed by using accurate multilevel fast multi-pole method (MLFMM), and application advices on near-field characteristics were given in Ref. [5]. The generalized radar cross section in the rear-field of target was computed after confirming the current and magnetic sources by the finite element method.^[6] The backward near-scattering field from missile target was calculated by using time-domain physical-optics method.^[7] All the above methods for near field have perfect accuracy and somewhat adequacy in solving the near-field scattering from target without rough surface. However, they could not be extended to solving the composite near-field EM scattering problems because of difficulties caused by high frequency and rough surface with extra electrically large size. Composite EM scattering from rough surface and target can be solved by various high-frequency analytical methods, such as physical optics method,

equivalent edge currents method, shooting and bouncing ray (SBR) and hybrid approximate method, *etc.* Enlightened by SBR in far-field conditions, we propose the modified SBR method combined with integral equation method (IEM) here based on previous research, in order to solve the near-field EM scattering problems of rough surface and target above it. And the near-field EM scattering characteristics of plane-water surface are analyzed in the simulation example.

2. Composite near-field EM scattering model of target in extra-low-altitude and environment

When radar detecting targets in extra-low-altitude as shown in Fig. 1, if the distance R between antenna and target satisfies the following condition:

$$R < 2D^2/\lambda, \quad (1)$$

where λ is the wave length, D is the maximum size of target in three dimension, then the target is in radiating near-field region of the horn, and the couple horn is also in scattering near-field region of scatters.

The path of EM wave propagation for near-field scattering is probably the same as that for far-field scattering, in which the main propagation paths contributing to scattering are classified as five types: horn-target/surface-horn, horn-target-surface-horn, horn-surface-target-horn, horn-target-surface-target-horn and horn-surface-target-surface-horn, and there may be even more complex paths with bouncing more than 3

*Project supported by the National Natural Science Foundation of China (Grant No. 61372033).

†Corresponding author. E-mail: bigboy11272000@126.com

times, if the target is hanged in a particular angle above the surface. Therefore, the SBR method can be used to describe the propagation process. However, there are differences between near-field situation and far-field situation as follows.

(i) The EM wave illuminating the target is not a plane wave any more.

(ii) Green's function has an approximate expression [formula (2)] which is suitable in far-field conditions, when calculating the scattering field caused by target surface currents,

$$G = \frac{e^{-jkR}}{R}, \quad (2)$$

where R is the distance between source point and observation point.

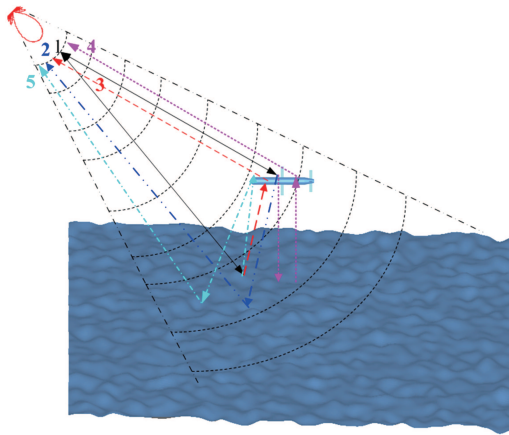


Fig. 1. Scene of composite scattering from target in extra-low-altitude and on rough surface.

3. Solution of composite near-field scattering model by modified SBR-IEM hybrid method

3.1. Modified principle of dividing ray tubes

In the conventional SBR method for far-field problems, the transmitting ray tubes are parallel to the propagating direction of the incident wave, on the assumption that the equivalent phase surface is a plane which all the transmitting ray tubes perpendicular to, and rays have the same original phase and amplitude as each other. However, the assumption about plane wave is not available in near-field condition. Therefore, the incident EM field must be described based on the near-field pattern of the antenna.

Determining the transmitting direction of ray tube is similar to simulating the equivalent phase surface of plane wave. Firstly, the virtual aperture plane is built, which is perpendicular to the line (the wide red solid line in Fig. 2) connecting the antenna and the target center, and the projection area of the box surrounding target on this virtual plane can be determined as a ray aperture, all above can be seen in Fig. 2. Secondly, in order to obtain reliable and convergent results, the modified SBR still adopts a rule of thumb in which the distance d between adjacent rays should be chosen to be $d \leq \lambda/10$, but rays

have not the same direction any more as the rays in conventional SBR, the real directions are determined by connecting antenna and points of divided grids in ray aperture as shown in Fig. 3.

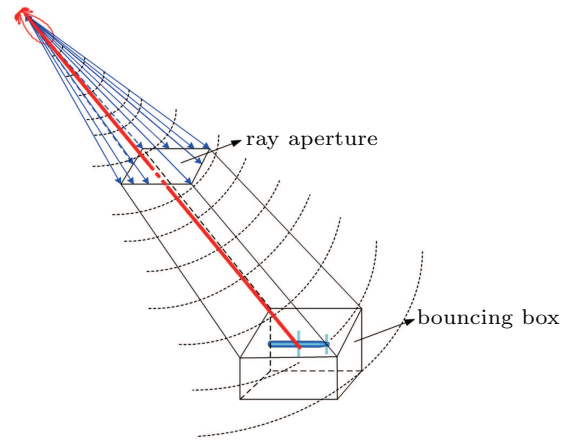


Fig. 2. Box surrounding target and virtual transmitting plane.

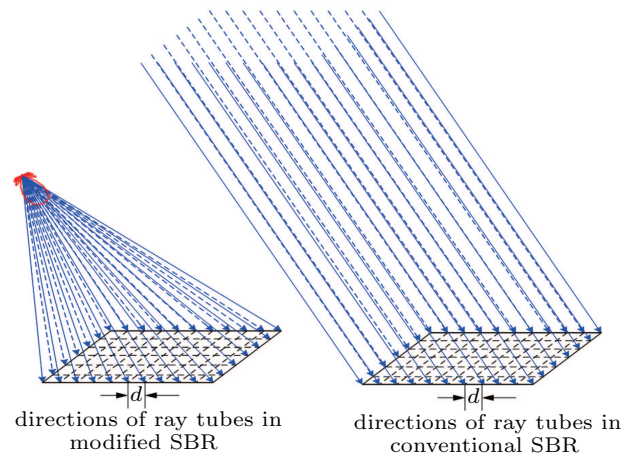


Fig. 3. Grids in ray aperture and directions of rays.

3.2. Modified Green's functions in near-field conditions

When the distance $|r - r'|$ does not satisfy $|r - r'| > 2D^2/\lambda$ in the near-field condition, great error may arise if Green's function is still calculated by formula (2). Although neither the whole target nor the observation point is under the far-field condition, each facet (S_n) of the target surface is much smaller than the whole profile of the target. So the distance between each facet and observation point $|r_n - r'|$ satisfies $|r_n - r'| > 2D_{S_n}^2/\lambda$, where r_n is the center vector of the n -th facet S_n , D_{S_n} is the scale of the n -th facet. The scattering direction \hat{k}^{sn} of facet S_n is not along \hat{R} ($\hat{R} = (r - r')/|r - r'|$), but should be

$$\hat{k}^{sn} = \frac{\mathbf{R}_n}{|\mathbf{R}_n|} = \frac{r - r_n^c}{|r - r_n^c|}, \quad (3)$$

where $\mathbf{R}_n = r - r_n^c$, and the incident direction \hat{k}^{in} can be written as $\hat{k}^{in} = -\hat{k}^{sn}$.

Then Green's function should be written as

$$G = \frac{e^{-jk\hat{R} \cdot (r - r')}}{R} \approx \frac{e^{-jk\hat{k}^{sn} \cdot (r - r')}}{r}. \quad (4)$$

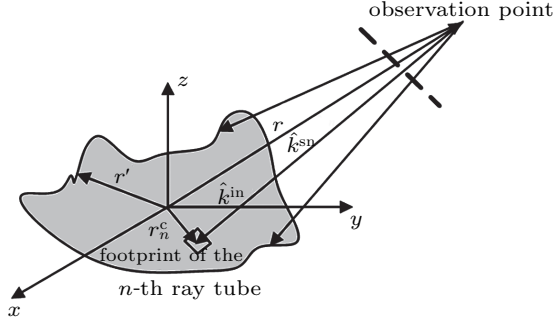


Fig. 4. Scattering direction of grid face in near-field condition.

3.3. Calculation of scattering from rough surface

Rough surface can be described by two-scale model, in which the global undulate profile is indicated by splitting rough surface with large facet elements, and the local statistical properties in each large facet is approximated by using the classical spectrum functions for rough surface.

3.3.1. Coherent scattering contribution of small scale model

The coherent scattering matrix $\bar{\bar{R}}_{\text{rough}}$ is modified with geometric optics reflection matrix \bar{R} for small flat facet element multiplied by the rough level factor $e^{-4k_n^2\sigma^2}$ determined by the roughness, and thus it can be written as

$$\bar{\bar{R}}_{\text{rough}} = e^{-4k_n^2\sigma^2} \cdot \bar{R}, \quad (5)$$

where k_n denotes the component of wave vector in the normal direction of the facet, and σ is the standard variance of rough surface height.

Then the coherent scattering field E_s^{n1} from the n -th rough facet can be calculated by $\bar{\bar{R}}_{\text{rough}}$ and incident field E_{in}^n

$$E_s^{1n}(\mathbf{r}) = e^{ikr} \bar{\bar{R}}_{\text{rough}} \cdot E_{\text{in}}^n, \quad (6)$$

where E_s^{n1} is produced by ray tube from target facet, and E_{in}^n can be calculated by the modified SBR method, after ray tracking between target and rough surface is finished,

$$E_{\text{in}}^n = \sum_{j=1}^M E_j^n, \quad (7)$$

where M is the total number of target facets, E_j^n is the incident field of the j -th target facet on the n -th rough facet, and it can be obtained after rays tracking has been accomplished.

And the total coherent scattering field from rough surface can be described as

$$E_s^1 = \sum_{n=1}^N E_s^{1n}, \quad (8)$$

where N is the total number of rough surface facets.

3.3.2. Incoherent scattering contribution of large scale model

The incoherent scattering component is the second-order moment of the random scattering field.^[8] The scattering matrix is derived from Mueller-matrix of rough surface as shown in the following formula:

$$[S_{\text{rough}}] = \bar{C}^{1/2} \cdot \bar{s}_0, \quad s_j^0 = a + ib, \quad j = 1, \dots, 4, \quad (9)$$

where $[S_{\text{rough}}]$ is the vector composed of the elements in the diffused scattering matrix $\bar{\bar{S}}_{\text{rough}}$, a and b are Gaussian random numbers with the zero mean and unit variance, and C is the covariance matrix of Mueller-matrix, and its lower triangular square root $\bar{C}^{1/2}$ can be obtained by Cholesky-decomposition.

Elements of Mueller-matrix are composed of the second-moment of scattering matrix elements, so only the second-moment of scattering-matrix elements is written below:

$$\langle S_{pq} S_{rs}^* \rangle = \frac{k^2}{8\pi} \exp[-\sigma^2(k_z^2 + k_{sz}^2)] \times \sum_{n=1}^{\infty} \sigma^{2n} (I_{pq}^n I_{rs}^{n*}) \frac{W^{(n)}(k_{sx} - k_x, k_{sy} - k_y)}{n!},$$

$$I_{pq}^n = (k_{sz} + k_z)^n f_{pq} \exp(-\sigma^2 k_z k_{sz}) + \frac{k_{sz}^n F_{pq} + k_z^n F_{pq}^s}{2}, \quad (10)$$

where $p, q, r,$ and s denote the subscript of polarization component h or v , the vertical polarization is simplified by v , the horizontal polarization by h , and the coefficients of Kirchhoff approximate scattering field have formulas below:

$$\begin{aligned} f_{vv} &= \frac{2R_v}{\cos \theta_i + \cos \theta_s} \\ &\times [\sin \theta_i \sin \theta_s - (1 + \cos \theta_i \cos \theta_s) \cos(\varphi_s - \varphi_i)], \\ f_{hh} &= \frac{2R_h}{\cos \theta_i + \cos \theta_s} \\ &\times [\sin \theta_i \sin \theta_s - (1 + \cos \theta_i \cos \theta_s) \cos(\varphi_s - \varphi_i)], \\ f_{hv} &= (R_h - R_v) \sin(\varphi_s - \varphi_i), \\ f_{vh} &= (R_v - R_h) \sin(\varphi_i - \varphi_s), \end{aligned} \quad (11)$$

where θ and φ are vertical angle and horizontal angle respectively, the subscripts i and s denote incident and scattering respectively. And the compensation coefficients are written as

$$\begin{aligned} F_{vv} &= -(cu_v - qt_v/\epsilon_r)(t_v c_d + u_v \epsilon_r c_1) + (v_v^2 - ct_v u_v/q) c_2^s, \\ F_{hh} &= (cu_h - qt_h)(t_h c_d + u_h c_1) - (v_h^2 - ct_h u_h/q) c_2^s, \\ F_{hv} &= (cu - qt/\epsilon_r)(t/c_s + u\epsilon_r/q) s_d - (u^2 - ct u/q) s^2 s_d, \\ F_{vh} &= (ct - qu)(u/c_s + tq) s_d + (t^2 - ct u/q) s^2 s_d, \\ F_{vs}^s &= -(c_s u_v - q_s t_v/\epsilon_r)(t_v c_d + u_v \epsilon_r c_1^s) + (t_v^2 - c_s t_v u_v/q_s) c_2^s, \\ F_{hs}^s &= (c_s u_h - q_s t_h)(t_h c_d + u_h c_1^s) + (t_h^2 - c_s t_h u_h/q_s) c_2^s, \\ F_{hv}^s &= -(c_s t - q_s u)(u/c_s + t/q_s) s_d - (u^2 - c_s t u/q_s) s^2 s_d, \\ F_{vh}^s &= -(c_s u - q_s t/\epsilon_r)(t/c_s + u\epsilon_r/q_s) s_d \\ &\quad - (t^2 - c_s t u/q_s) s^2 s_d. \end{aligned} \quad (12)$$

And the parameters in formula (12) can be written as follows:

$$\begin{aligned}
 s &= \sin \theta_i, \quad s_s = \sin \theta_s, \quad s_d = \sin(\varphi_s - \varphi_i), \\
 c &= \cos \theta_i, \quad c_s = \cos \theta_s, \quad c_d = \cos(\varphi_s - \varphi_i), \\
 q &= \sqrt{\varepsilon_r - \sin^2 \theta_i}, \quad q_s = \sqrt{\varepsilon_r - \sin^2 \theta_s}, \\
 c_1 &= \frac{c_d - s s_s}{q c_s}, \quad c_1^s = \frac{c_d - s s_s}{q_s c}, \\
 c_2 &= s \frac{s_s - s c_d}{c_s}, \quad c_2^s = s_s \frac{s - s_s c_d}{c}, \\
 t_v &= 1 + R_v, \quad t_h = 1 + R_h, \quad t = 1 + (R_v - R_h)/2, \\
 u_v &= 1 - R_v, \quad u_h = 1 - R_h, \quad u = 1 - (R_v - R_h)/2, \\
 k_x &= k \sin \theta_i \cos \varphi_i, \quad k_y = k \sin \theta_i \sin \varphi_i, \quad k_z = k \cos \theta_i, \\
 k_{sx} &= k \sin \theta_s \cos \varphi_s, \quad k_{sy} = k \sin \theta_s \sin \varphi_s, \quad k_{sz} = k \cos \theta_s. \quad (13)
 \end{aligned}$$

Then the diffused scattering component E_s^2 from ray tube on each cross between reflecting path and facet can be expressed by the product of diffused scattering matrix $\bar{\bar{S}}_{\text{rough}}$ and E_i as follows:

$$E_s^2(\mathbf{r}) = e^{ikr} \bar{\bar{S}}_{\text{rough}} \cdot E_i. \quad (14)$$

The total scattering field from each facet is the sum of coherent component and incoherent component as expressed below:

$$E_s = E_s^1 + E_s^2. \quad (15)$$

It is emphasized that the Monte–Carlo simulation for producing rough surface is done repeatedly many times in order to obtain the mean results, and the Gaussian random number for each grid facet should be consistent in each simulation.

During the Monte–Carlo simulations, the target facets and rough surface facets should be treated by using different rules after rays tracking between target and rough surface has been finished. The rules are that the scattering from target facets are calculated only once, but those for rough surface facets are implemented many times. Finally, the composite scattering field is the sum of scattering field from target and the mean of multiple scattering fields from rough surface.

4. Numerical examples for composite near-field EM scattering

4.1. Numerical validations

Example 1 As shown in Fig. 5, a PEC plate with a side length of 0.6 m is set to be above water surface perpendicular to the plate, and the distance between water and the lower side of the plate is 0.1 m. The frequency of incident wave is 10 GHz with VV polarization, and the main beam width of the horn is 13° , the testing distance between the plate and horn is set to be 13 m. The area of the truncated water surface is $5 \text{ m} \times 5 \text{ m}$, and the root mean square (RMS) value of water surface height is about 0.01 m.

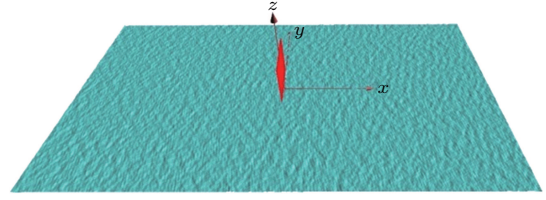


Fig. 5. Plate and water surface below.

Figure 6 shows both the composite near-zone radar cross section (RCS) of plate–water and laboratory measurements, it can be found that they are basically in accord with each other.

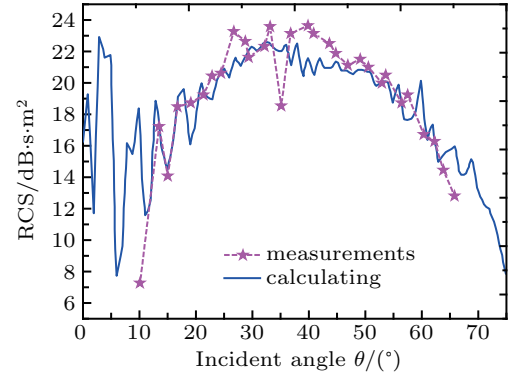


Fig. 6. Comparisons between numerical results of the plate–water surface by modified SBR-IEM and measurements.

Example 2 As shown in Fig. 7, a PEC ladder-shaped block is set to be above water surface. The size of the block bottom is $0.9 \text{ m} \times 1.35 \text{ m}$, and its top is a square of $1.35 \text{ m} \times 1.35 \text{ m}$. The distance between water and block bottom is 0.1 m. The parameters for horn and incident wave are the same as those in example 1. And the testing distance is 10 m. The calculated results are approximately equal to the measured data.

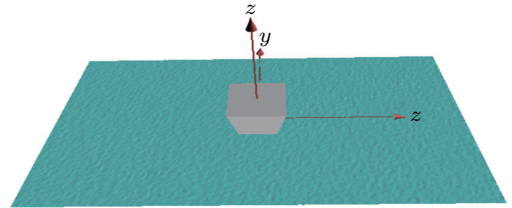


Fig. 7. Ladder-shaped block and water surface.

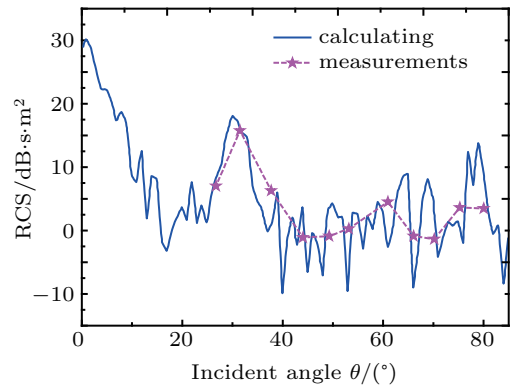


Fig. 8. Comparison between numerical results of the block–water surface and measurements.

4.2. Analysis of near-zone composite scattering from plate and water surface

In order to reveal the multiple scattering between target and surface below, the slanted angle between plate and water is 30° as shown in Fig. 9, and the plate side width is 0.6 m. The plate supported by a thin bar is 2.1 m above the water surface. The observation horn is at the altitude of 4.1 m. The angle between main beam and water surface is 60° , other parameters are the same as those in example 1. Moving the observation horn to the target along the horizontal direction, the near-zone composite RCS *versus* the changing horizontal distance between horn and target is obtained both by numerical calculation and by laboratory measurement. Comparison of the two results is firstly given in Fig. 10, showing that they have the same tendency and amplitude. Particularly, when the horizontal distance is around 3.8 m, the composite multiple scattering between the plate and water surface reaches a maximum value, while the second maximum value of RCS appears at a distance of 1.3 m where the direct scattering from target is relatively weak. What is more, the RCS line has double peak at 1.3 m, this is because the back of the plate is supported by a thin bar. And the average RCS error between measurements and calculations is more than 2 dB in the area of multiple scattering existing.

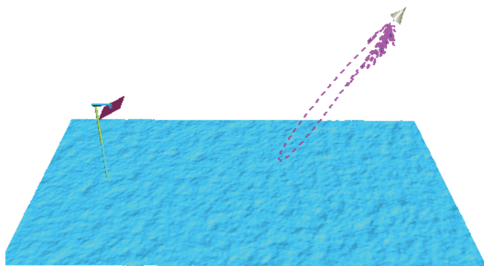


Fig. 9. Composite scattering from slanted plate and water surface.

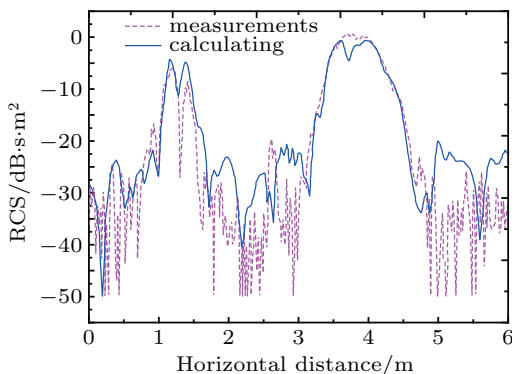


Fig. 10. Comparison between measured and calculated near-zone RCS *versus* the horizontal distance between observation horn and target.

In the next numerical example, the near-zone composite scattering from a missile and ocean rough surface below is considered, which is shown in Fig. 11. The simulation parameters are set to be as follows. The incident frequency is

10 GHz with VV polarization, the missile is parallel to the +X axis, the wind speed above the ocean is 5 m/s, the height of the missile is 5 m above the surface, missile length is 2.57 m, missile diameter is 0.52 m, missile wing span is 2.65 m, ocean surface size is 24 m×24 m, and the ocean is not supposed to be PEC any more, the relative dielectric parameter of common ocean surface is set to be $60 + j32$ according to double Debye model.^[9] The near-zone composite scattering is solved by using the proposal hybrid method and MLFMM. The RCS results are displayed in Fig. 12. The accuracy of the hybrid method is proved by comparing with MLFMM, with the simulating step set to be 5° because of its time consuming.

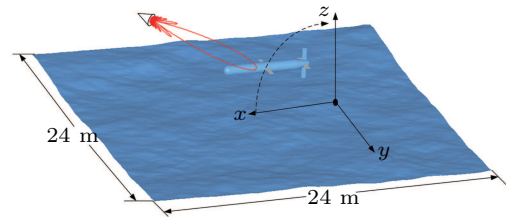


Fig. 11. Composite scattering from missile and ocean surface.

By analyzing RCS tendency displayed in Fig. 12, the near-field scattering from missile and ocean surface achieves the peak value when they are illuminated vertically (around 0°), and the second peak value appears when illuminated horizontally (around 90°). This is because the coherent scattering component (mirror scattering from ocean surface) makes the main scattering contribution when incident wave is vertical to the ocean surface, and the incoherent scattering component rises as the incident angle increases, while the coherent scattering turns weaker. The second scattering peak is caused by scattering from the warhead of missile.

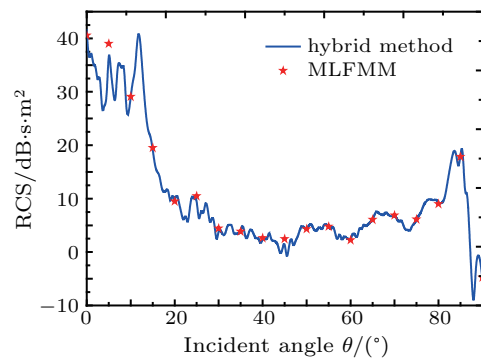


Fig. 12. Comparison between near-zone RCSs of missile and ocean surface *versus* incident angle, obtained by proposal hybrid method and MLFMM.

5. Conclusions and perspectives

A novel hybrid method is proposed to solve the near-zone composite scattering from target in extra-low-altitude and extra electric large rough surface. The conventional SBR method and IEM are modified in accordance with the physical mechanism in near-zone composite scattering problems, and the

new hybrid method, called modified SBR-IEM, is established. By comparing the simulated results of the modified SBR-IEM with measured results, the accuracy of the proposed method is testified by two numerical examples. And then the near-zone composite scattering characteristics are analyzed by hanging a slanted plate above the slight rough water surface, the variation of near-zone RCS with near-field distance is obtained finally. However, the proposed method is suitable only for the PEC targets and rough surface. In order to extend the applicability of the hybrid method, the physical optics (PO) scattering field formula must be modified to conform to the situation of dielectric and dielectrically coated targets, which is the key problems we will pursue in the future. Finally, the proposed method can be generalized to solving the near-zone compos-

ite scattering from targets with complex geometric structures and sea/ground surface, and may have great practical value in missile-borne radar detecting and near-zone scattering problems for fuzes.

References

- [1] Zhang D M, Liao C, Zhou L, Deng X C and Feng J 2018 *Chin. Phys. B* **27** 074102
- [2] Xu R W, Guo L X and Wang R 2014 *Chin. Phys. B* **23** 114101
- [3] Johnson J T 2002 *IEEE Trans. Geosci. Remote Sens.* **50** 1361
- [4] Johnson J T 2001 *Microwave Opt. Technol. Lett.* **30** 130
- [5] Su J S and September Z P 2014 *Acta Electronica Sin.* **42** 1823
- [6] Gao H W, Gong L and Sheng X Q 2014 *January Transactions Beijing Institute and Technology* **34** 88
- [7] Guo G B and Guo X L 2017 *Chin. J. Radio Sci.* **32** 385
- [8] Xu F and August Y Q 2006 *IEEE Trans. Geosci. Remote Sens.* **44** 3219
- [9] Meissner T and Wentz J 2004 *IEEE Trans. Geosci. Remote Sensing* **42** 1836